Journal of Applied Polymer Science

Poly(vinyl alcohol)/Cu(II) Complex Anion Exchange Membranes Prepared Using Chemical Fiber for Direct Methanol Fuel Cells

Pei Yu Xu, Chun Hui Zhao, Qing Lin Liu
Department of Chemical and Biochemical Engineering, College of Chemistry and Chemical Engineering, Xiamen University, Xiamen 361005, People's Republic of China
Correspondence to: Q. L. Liu (E-mail: qlliu@xmu.edu.cn).

ABSTRACT: PVA/Cu (II) complex anion exchange membranes (AEMs) were prepared for direct methanol fuel cells. The complex was for the first time used as membrane material of AEMs. Glutaraldehyde as a crosslinking agent was introduced to control water uptake and swelling of the membranes. The membranes with thickness of 1 μm were fabricated using chemical fibers based on the solution surface tension. The complex membranes show good ionic conductivity and low methanol permeability in the magnitude of 10^{-2} $S \cdot cm^{-1}$ and 10^{-7} $cm^{-2} \cdot S^{-1}$, respectively. This is a facile, efficient, green, and fast way to prepare new AEMs for direct methanol fuel cells. © 2013 Wiley Periodicals, Inc. J. Appl. Polym. Sci. 130: 1172–1178, 2013

KEYWORDS: membranes; films; composites

Received 13 November 2012; accepted 18 March 2013; Published online 17 April 2013
DOI: 10.1002/app.39294

INTRODUCTION

Direct methanol fuel cells (DMFCs) are developed from proton exchange membrane fuel cells (PEMFCs) in which methanol is used as the fuel. Their main advantages include ease of transportation and storage of the fuel, high energy efficiency, and high power density.[1,2] Polymer electrolyte membrane is one of the most important components in DMFCs and greatly influences their performances. Therefore, good performance of DMFCs is heavily dependent on the polymer electrolyte membranes. Proton exchange membranes (PEMs), in particularly, Nafion membranes have been widely used in DMFCs and exhibited excellent thermal and chemical stability and ionic conductivity. However, some flaws still exist in PEMs and hinder the development of DMFCs. The main problems include: (1) high methanol permeability, (2) slow methanol oxidation kinetics at the anode, (3) CO poisoning of catalysts at low temperature, and (4) severe electro-osmosis of water from the anode to the cathode.[3–5] Anion exchange membranes (AEMs) have thus attracted significant interests because they have better kinetics of the oxygen reduction reaction and catalytic activities and lower methanol permeability in alkaline media.[5,6] As a result, high performance of AEMs is the key to the success in DMFCs.

The property of AEMs depends on membrane materials. In the past years, AEM materials focus on the modification of commercial polymers via chemical reaction including poly(sulfone)s,[7,8] ploy(phthalazinone ether sulfone ketone),[9] poly(ether imide),[10] poly(phenylene oxide),[11,12] and poly(vinyl acetate).[13–15] Membrane materials are still under development by now with the aim of achieving improved membrane property over Nafion membranes. The complexes of polymers and metal salt have been researched for years. Incorporation of the plastics or inorganic metal salt into the conducting polymers is an attractive route in improving the processability without losing mechanical properties. At the same time, incorporation of a transition metal ion into the organic compound is generally found to enhance its stability.[16] However, this kind of polymer–metal salt complexes has not been used as membrane materials. Therefore, complex of poly(vinyl alcohol) (PVA)/$Cu(NO_3)_2$ was prepared and used as membrane materials for the first time in this work. PVA is a low-cost hydrophilic polymer and has high water selectivity to alcohols. It exhibits low methanol permeability and has been used in some alkaline fuel cells. Therefore, the problem of high methanol crossover could be resolved using this membrane material. Cu ion in the $Cu(NO_3)_2$ and the hydroxyl on the PVA chain can form PVA/Cu complex structure material with improved performance over the pristine PVA membranes. Glutaraldehyde (GA) is introduced during membrane preparation to crosslink PVA for controlling the swelling and water uptake of the membranes. Our previous work showed that the water uptake and swelling of the membranes decreased with increasing the amount of GA.[13]

Additional Supporting Information may be found in the online version of this article.

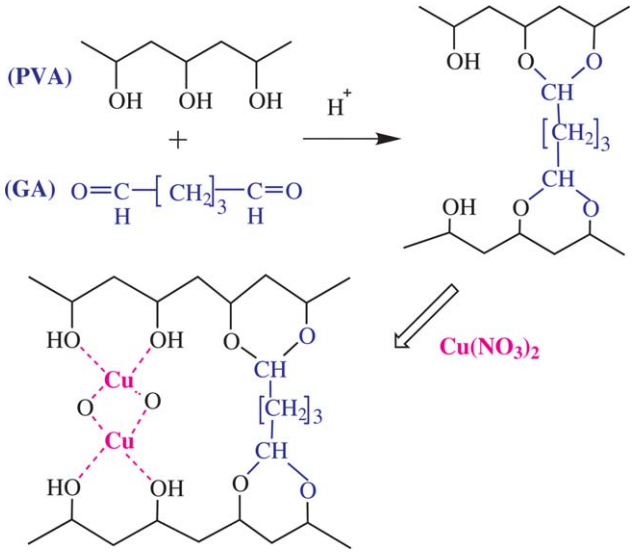

Scheme 1. The schematic of PVA/Cu complex. [Color figure can be viewed in the online issue, which is available at wileyonlinelibrary.com.]

Typically, there are two ways to synthesize polymer membrane materials. One is to modify commercial membrane materials. The other is to design and synthesize novel structural polymers. However, some limitations are encountered in both the two ways. These include (1) amount of organic solvent such as dimethyl sulfoxide (DMSO) is used during preparation, (2) quaternary ammonium salt of reagent such as trimethylamine harmful to the human body and the environment is to be added, (3) the process for membrane fabrication is tedious. Therefore, to develop a new and green way in the preparation of polymer membranes is important.

Surface tension is the property of the liquid surface that allows it to resist an external force and to hold the liquid film. The surface tension of the membrane casting solution can be used for the preparation of thin membranes. As long as the casting solution has a sufficient polymer concentration, the surface tension can support the weight of solution to hold it together. Chemical fiber has been introduced into the novel facile process for membrane preparation. A thin liquid film could be formed by passing the chemical fiber through the casting solution on the basis of the surface tension of solution. Meanwhile the solid electrolyte membrane can be formed in several hours at room temperature. The thickness of the as-prepared membranes around 1 μm is generally smaller than that of membranes fabricated by plate casting. Therefore, the novel facile way for membrane preparation has several advantages including: (1) membrane thickness is smaller than the reported AEMs, (2) the time for the facile process can be greatly shortened, and (3) the preparation does not need the assistance of organic solvents. Meanwhile, this way can also be a batch processing in preparing thin membranes.

EXPERIMENTAL

Preparation of PVA/Cu (II) Membranes

The synthesis of crosslinking polymer and the preparation of PVA/Cu(II) complex are shown in Scheme 1. GA was introduced into the solution to crosslink PVA that was dissolved in deionized water. The crosslinking reaction occurred at a pH of 5. The PVA/Cu(II) complex was formed after $Cu(NO_3)_2{\cdot}3H_2O$ being added to take the chemical reaction. The membrane prepared using chemical fiber is relied on the surface tension of the solution. The solution containing 0.8 mL of GA in 20 mL of PVA solution was used on the basis of previous research.[13] Therefore, 0.8 mL of GA was used in the present work.

A total of 0.50 g of PVA (1750 ± 50) was dissolved in 9.50 g of deionized water at 90°C for 4 h to prepare PVA solution. The solution was then cooled down to room temperature and placed statically for more than 12 h. 0.5*M* H_2SO_4 was used to adjust the pH of the PVA solution. After pH of 5 being achieved, 0.8 mL of GA (10 wt %) was added into the PVA solution with magnetic string for 2 h and placed statically for more than 12 h. Afterwards, 0.50 g of $Cu(NO_3)_2 \cdot 3H_2O$ was added into the solution under magnetic string for 2 h to form PVA/Cu complex solution. A liquid complex film can be formed after the chemical fiber going through the solution. The liquid film was dried at room temperature for 12 h and in a vacuum oven at 60°C for more than 4 h to yield the PVA/Cu complex membrane.

Characterization

UV–Visible. UV–visible (UV–vis) absorption of different solutions was measured using double-beam UV-spectrophotometer (TU-1900, Beijing Purkinje General Instrument) within the scanning range 190–900 nm.

Morphology and Microstructure of the Membranes. The morphology of the membranes was characterized using field emission scanning electron microscope (Hitachi S-4800, Japan). Before observations, the membranes were fractured in liquid nitrogen and then sputtered with gold. The microstructure of the membranes was characterized using transmission electron microscope (TEM-2100, Japan).

Thermal Stability. Thermal stability of the membranes was measured using a thermogravimetric analyzer (TG209F1, NETZSCH, Germany) under air atmosphere from 30°C to 800°C at a heating rate of 10°C min^{-1}.

Water Uptake and Membrane Swelling. Water uptake was determined by measuring the difference in weight of the membrane before and after being immersed in deionized water. The membrane sample was first placed in deionized water at 30°C for more than 24 h, and immediately weighed to measure the weight of the wet membrane after removing the surface water. Then the wet membrane was subsequently dried at 80°C under vacuum until a constant weight. The water uptake W_u (%) can be calculated by

$$W_u = \frac{m_w - m_d}{m_d} \times 100\% \quad (1)$$

where m_w and m_d are the mass of the wet and the dried membranes (g), respectively.

The swelling of membranes was measured in the plane direction, as characterized by

$$Swelling = \frac{L_s \times W_s - L_d \times W_d}{L_d \times W_d} \times 100\% \quad (2)$$

where L_s and L_d are the length of the wet and the dried membranes, respectively; W_s and W_d are the width of the wet and the dried membranes, respectively.

Ionic Exchange Capacity. Ionic exchange capacity (IEC) was measured using the classical back titration method. The weight of the dried membrane was first obtained. Then the membrane was soaked into a 10 mL of 0.1*M* HCl solution for 24 h to ensure an ionic exchange. The solution together with the membrane was back titrated with a 0.05*M* NaOH solution. The IEC values (mmol·g^{-1}) can be calculated by

$$IEC\left(meq \cdot g^{-1}\right) = \frac{M_{o,HCl} - M_{e,HCl}}{m_d} \quad (3)$$

where $M_{o,HCl}$ and $M_{e,HCl}$ are the milliequivalents (mmol) of HCl required before and after equilibrium, respectively.

Ionic Conductivity. Before test, the membrane was placed in deionized water for more than 48 h. The membrane was then cut into a rectangular strip (length: 2 cm, width: 1 cm) for conductivity measurement. The ionic conductivity of the membranes in the transverse direction was measured by two-probe AC impedance spectroscopy using a Parstat 263 electrochemical equipment (Princeton Advanced Technology, USA).[1] The impedance measurement was carried out over the frequency range $0.1-10^5$ Hz within the temperature range 30−70°C. The ionic conductivity σ (S·cm^{-1}) can be calculated by

$$\sigma = l/(AR_m) \quad (4)$$

where l is the distance between the two electrodes (cm), A the cross-sectional area of the testing membrane (cm^2), and R_m the membrane resistance (Ω) acquired from a Nyquist plot.

Methanol Permeability. The methanol permeability was measured within the temperature range 30−70°C using a homemade diffusion cell consisting of two identical diffusion compartments (refered to as A and B) with volume of approximately 25 cm^3.[1] Compartments A and B contained deionized water and 2*M* methanol aqueous solution, respectively. The variation of methanol concentration with time was measured by gas chromatography (GC-950, Shanghai Haixin Chromatographic Instruments). Assuming a pseudo-steady-state condition and $C_B \gg C_A$, the methanol permeability P (cm^2·s^{-1}) can be estimated as follows[1]:

$$C_A(t) = C_B\left(\frac{A_m}{l_m}\right)\left(\frac{P}{V_A}\right)(t - t_0) \quad (5)$$

where C_A and C_B are the concentration of methanol in compartments A and B (*M*), respectively, V_A the volume of the solution in compartment A (cm^3), l_m the membrane thickness (cm), A_m the effective area of the membrane (cm^2), and $(t-t_0)$ is the time used for methanol permeation testing.

X-ray Diffraction and Small Angle X-ray Scattering. The X-ray diffraction (XRD) of different membranes was measured using XRD (Rigaku, Ultima IV, Japan) within the scanning range 5−90°. The small angle X-ray scattering of different membranes was measured using small angle X-ray scattering (SAXS) (SAXSess-mc2, Anton Paar, Austria) within the scanning range 0−10°.

Alkaline Stability Testing. The alkaline stability of PVA/Cu(II) AEMs was investigated by conditioning the membranes in different KOH concentrations at 60°C for 48 h. Both IEC and ionic conductivity of the treated membranes were measured.

RESULTS AND DISCUSSION

The formation of PVA/Cu(II) complex solution is shown in Scheme 1.

UV–Visible

The complex was confirmed by UV–vis absorption spectra. Figure S1 (ESI) shows the UV–vis absorption curve of $Cu(NO_3)_2$, KNO_3, and $CuSO_4$ aqueous solutions. The absorption peak of Cu (II) ion and nitrate ion can thus be determined. Two peaks appeared near 300 and 800 nm in the absorption curve of $Cu(NO_3)_2$ aqueous solution. Only one peak near 300 nm can be observed in the curve of KNO_3 aqueous solution, meanwhile single peak near 800 nm can be found in the spectra of $CuSO_4$ aqueous solution. Therefore, the sharp peak at 300 is associated with nitrate ion, whereas the broad peak at 800 nm is associated with Cu (II) ion as noted by Ramya.[17]

Figure 1 shows the absorption curve of pristine PVA (1 wt %), $Cu(NO_3)_2$ (1 wt %) and PVA/Cu (II) complex (1 wt %) aqueous solutions. The peak at 190 nm is associated with PVA that can be observed in the pristine PVA aqueous solution. This absorption peak may be attributed to the n→σ^* transition that is very sensitive to hydrogen bonding. The absorption peak around 300 nm of PVA/Cu (II) complex aqueous solution can be attributed to the n→π^* transition and shifts to the right against PVA and $Cu(NO_3)_2$ aqueous solutions. It reveals that the micellar in the PVA/Cu complex aqueous solution is larger than that in the other two reagent aqueous solutions. This suggests the successful formation of complex structure between PVA and Cu ion. Figure S2 (ESI) shows the UV–visible

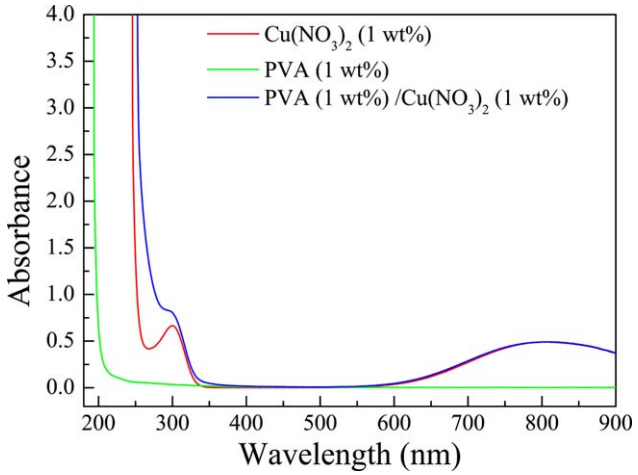

Figure 1. The UV–visible absorption curve of pristine PVA, $Cu(NO_3)_2$, and PVA/Cu(II) complex aqueous solutions. [Color figure can be viewed in the online issue, which is available at wileyonlinelibrary.com.]

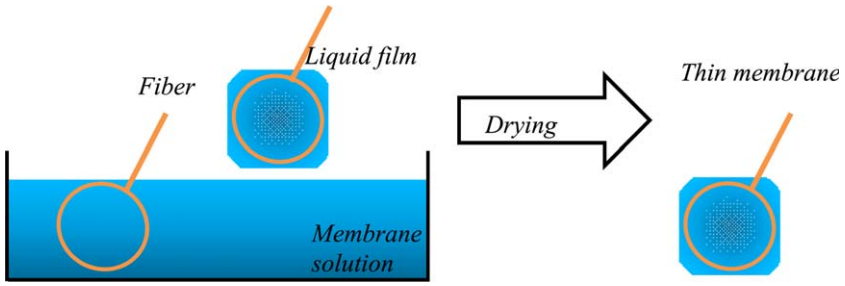

Scheme 2. The schematic of membrane preparation using chemical fiber. [Color figure can be viewed in the online issue, which is available at wileyonlinelibrary.com.]

absorption spectra with various Cu ion contents in the complex solution. The peak around 300 nm shifts to the right with increasing $Cu(NO_3)_2$ content. This indicates Cu ion connecting more PVA chains, as a result, more PVA/Cu(II) complex micellar has been formed with increasing Cu ion content. Therefore, the larger size of complex micellar has been observed at higher Cu content.

Membrane Preparation

A new developed method for membrane fabrication is shown in Scheme 2. Figure 2 shows the structure of chemical fiber (top) and the membrane (bottom) fabricated using the chemical fiber. There are three steps to prepare the membranes: (1) the chemical fiber is first put into the complex solution; (2) the chemical fiber is then pulled out carefully and the liquid film will be formed on the chemical fiber; and (3) the liquid film is finally dried to form the membranes. The membrane size and shape can be controlled by adjusting the overall dimension of the chemical fiber. Therefore, preparation of large area membranes can be fulfilled successfully on condition that the membrane solution has sufficient viscosity and surface tension. A liquid film can be formed on the chemical fiber. Therefore, thin membranes could be achieved using this kind of method. This way thus presents a facile, efficient, fast, and green route to fabricate thin AEMs.

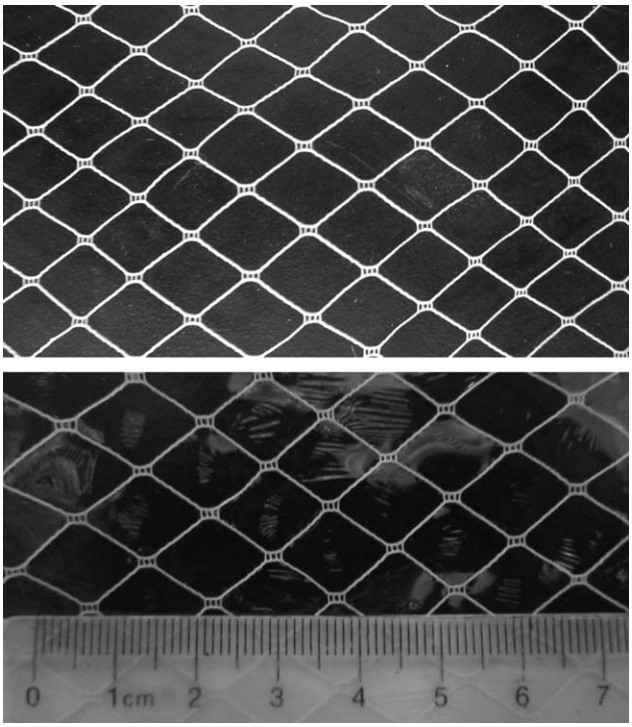

Figure 2. The feature of the chemical fiber (top) and the membrane (bottom) fabricated using the chemical fiber.

Water Uptake, IEC and Swelling of Membranes

PVA is a strong hydrophilic polymer. Therefore, GA was used as a crosslinking agent to control water uptake and swelling of the membranes. After being crosslinked by GA, water uptake of the crosslinked PVA membrane was 106.96% (Table I). The crosslinked structure of PVA has depressed water uptake. Meanwhile the water uptake of the PVA/Cu membrane decreased with the addition of Cu. This is partly owing to a similar crosslinked structure formed by Cu(II). As shown in Table I, the water uptake of PVA/Cu (5 wt %) and PVA/Cu (10 wt %) was 70.27% and 90.97%, respectively. The water uptake of the membranes increased with increasing Cu ion content but was still lower than that of the GA crosslinked PVA membranes without Cu ion. This is probably that the crosslinked structure is dominant in spite of the hydrophilicity of Cu ion.

The IEC of the two membranes was 0.676 and 0.960 $mmol \cdot g^{-1}$ accordingly. As shown in Figure S3 (ESI), the swelling of the pristine PVA membrane is 85.13%. The swelling ratio of PVA/GA and PVA/GA/Cu membranes is 65.64% and 31.54%, respectively. The result is partly because of the crosslinked structure.

Ionic Conductivity

The low ionic conductivity exhibited by AEMs hinders the development of AEM-DMFCs. The PVA/Cu(II) complex AEMs show a good ionic conductivity in the magnitude of 10^{-2} $S \cdot cm^{-1}$ and the highest one is 9.94×10^{-2} $S \cdot cm^{-1}$ at 70°C with 10 wt % Cu. At 30°C, the ionic conductivity of PVA/Cu(II) complex AEMs with 1 wt % Cu still showed a good ionic conductivity of 2.77×10^{-2} $S \cdot cm^{-1}$, whereas was 0.94×10^{-2}

Table I. The Water Uptake and IEC of the As-Prepared Membranes

	Water uptake (%)	IEC ($mmol \cdot g^{-1}$)
GA crosslinked PVA	106.96	NA
PVA/Cu (II) (5 wt %)	70.27	0.676
PVA/Cu (II) (10 wt %)	90.97	0.960

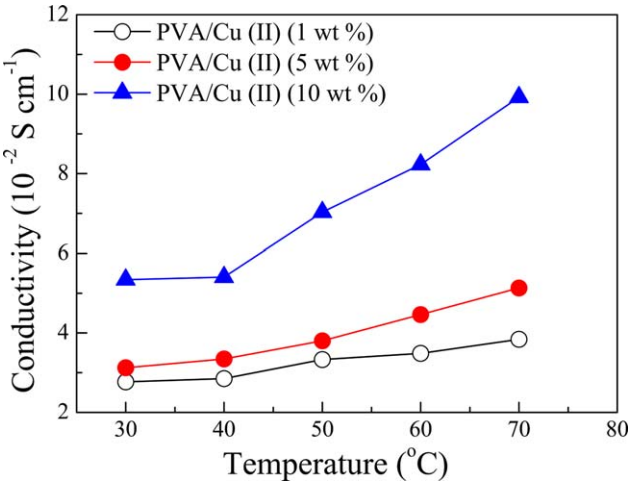

Figure 3. The ionic conductivity of the as-prepared membranes. [Color figure can be viewed in the online issue, which is available at wileyonlinelibrary.com.]

S·cm^{-1} for Nafion® 115.[18] As shown in Figure 3, the ionic conductivity increased with increasing temperature. Meanwhile, the ionic conductivity enhanced by increasing Cu ion content. This suggests that Cu (II) could be considered as ion exchange active sites to attract anion and form an ion transport channel. Therefore, the high conductivity of complex membranes is resulting from the high complex structure. The ionic conductivity increased with increasing temperature because the water diffusion and ionic conductance enhanced at a high temperature.

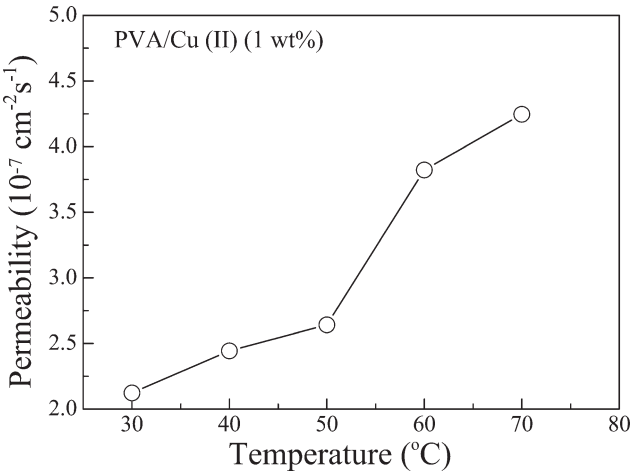

Figure 4. The methanol permeability of the as-prepared membranes.

Methanol Permeability

Methanol permeability is a serious issue that needs to be resolved in DMFCs. As shown in Figure 4, the methanol permeability of the as-prepared membranes is in the magnitude of 10^{-7} cm^{-2}·S^{-1} and the lowest one is 2.12×10^{-7} cm^{-2}·S^{-1} at 30°C, whereas it is 3.15×10^{-6} cm^{-2}·S^{-1} for Nafion® 115.[18] The complex membranes show low methanol crossover against Nafion membranes. The polymer material property and crosslinked structure should be responsible for the results. PVA has good methanol resistance. Meanwhile, the as-prepared membranes tended to be more compact and the interchain spacing thus reduced after being crosslinked by GA. Therefore, this leads to low methanol permeability.

SEM and Transmission Electron Microscope

As shown in Figure 5, the SEM image of cross section of the as-prepared membrane is homogenous, and the thickness of 1 μm is determined by SEM. The membrane is compact and smooth. Therefore, the catalytic effect will be the highest with the maximum interface contact area between the membrane and the catalyst layer. Figure S4 (ESI) shows the microstructure of the as-prepared membrane by TEM. Thin membrane without special structure can be noted. However, some small particles can be observed on the side of membrane. The small black particles may be associated with nano-Cu resulting from the reduction of Cu ion by hydroxyl on PVA chain during the sample preparation.

XRD and SAXS

Figure S5 (ESI) shows the XRD of two different membranes. A sharp peak near 20° can be observed clearly in the pristine PVA membrane. However, the intensity of peak near 20° in the XRD of PVA/Cu membrane decreased remarkablely. The obvious difference in crystallization of PVA is because of the complex reaction and crosslinking. The good ionic conductivity is also originated from the amorphous area of membrane material. Figure 6 shows the SAXS of the two different membranes. A

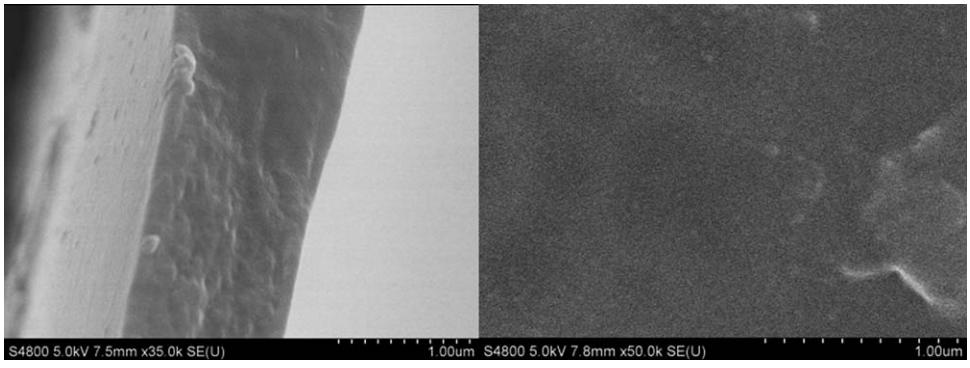

Figure 5. The SEM images of the PVA/Cu (II) (5 wt %) membrane: cross section (left) and surface (right).

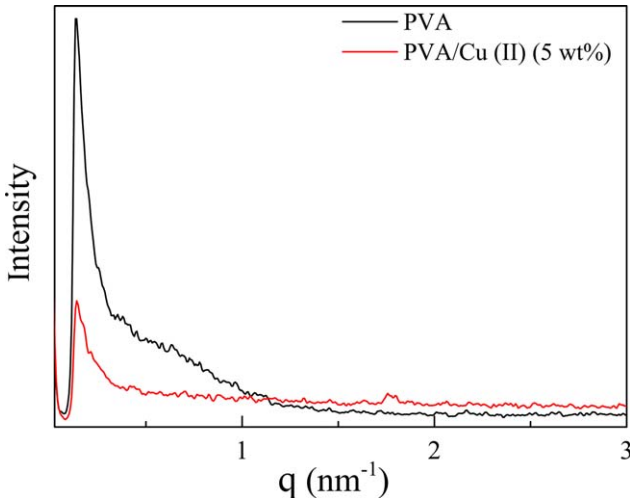

Figure 6. The SAXS curves of the GA crosslinked PVA and PVA/Cu(II) (5 wt %) complex membranes. [Color figure can be viewed in the online issue, which is available at wileyonlinelibrary.com.]

peak near 0.2 nm^{-1} can be observed clearly. The intensity of PVA/Cu complex membrane is lower. This suggests the PVA interchain spacing decreased and larger PVA/Cu complex micellar was formed in the membrane.

TGA

Figure 7 shows the thermal stability of this complex membrane. All the membranes exhibit three thermal decomposition steps under air atmosphere. The first step from 30°C to 150°C is associated with evaporation of water. The marginal weight loss from 150°C to 250°C is attributed to the degradation of the crosslinked structure formed in the membranes. The third step starting from 250°C to 500°C is because of the cleavage of the polymer backbone. The ultimate degradation temperature of membranes decreased with increasing Cu ion content. This suggests the existence of metal in the polymer could reduce the thermal stability of membrane. This kind of membrane is found to have good thermal stability under 100°C. The results should be improved when tested under nitrogen atmosphere in which the thermal stability evaluation is normally performed in the literature.

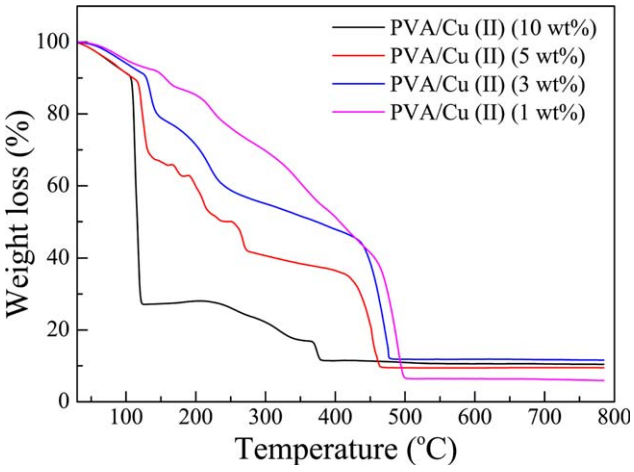

Figure 7. The TGA curves of the PVA/Cu(II) complex membranes with various Cu ion contents. [Color figure can be viewed in the online issue, which is available at wileyonlinelibrary.com.]

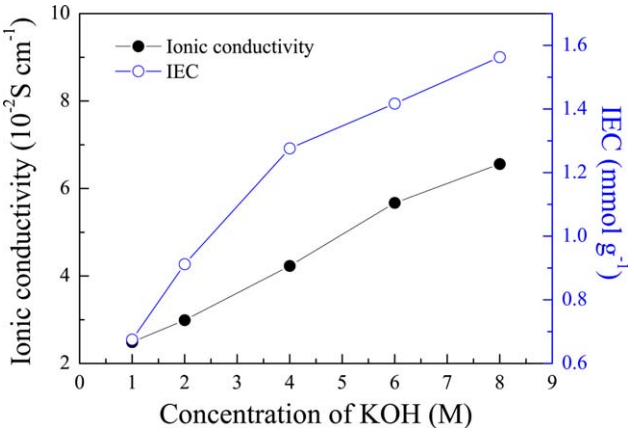

Figure 8. IEC and ionic conductivity (at 60°C) of the PVA/Cu(II) (5 wt %) membranes after treated with KOH solution with different concentrations at 60°C for 48 h. [Color figure can be viewed in the online issue, which is available at wileyonlinelibrary.com.]

Alkaline Stability of PVA/Cu(II) AEMs

Figure 8 shows both IEC and ionic conductivity of the treated membranes improved with increasing KOH concentration. This suggests that Cu (II) could attract more OH^- to form a desirable ion transport channel, which facilitates the transfer of OH^- in alkaline solution with higher KOH concentration. The membrane immersed in alkaline solution can keep high IEC and ionic conductivity. This suggests the PVA/Cu(II) AEMs being stable to some extent.

CONCLUSIONS

PVA/Cu(II) complex AEMs are prepared successfully in this article for the first time. GA as a crosslinking agent has been introduced to control water uptake and swelling of the membranes. The thin membranes can be fabricated using chemical fiber based on the solution surface tension. The complex membranes in the thickness of 1 μm show good ionic conductivity and low methanol permeability in the magnitude of 10^{-2} $S{\cdot}cm^{-1}$ and 10^{-7} $cm^{-2}{\cdot}S^{-1}$, respectively. This is a facile, efficient, green and fast way to prepare new AEMs for direct methanol fuel cells.

ACKNOWLEDGMENT

Financial support from National Nature Science Foundation of China Grant Nos. 20976145,21076170 and 21107089, Nature Science Foundation of Fujian Province of China Grant Nos.2009J01040 and 2011J01055, and the research fund for the Doctoral Program of Higher Education (Nos. 20090121110031 and 20110121120041) in preparation of this article are gratefully acknowledged.

REFERENCES

1. Guo, T. Y.; Zeng, Q. H.; Zhao, C. H.; Liu, Q. L.; Zhu, A. M.; Broadwell, I. *J. Membr. Sci.* **2011**, *371*, 268.
2. Heinzel, A.; Barragán., V. M. *J. Power Sources* **1999**, *84*, 70.

3. Wasmus, S.; Kuver, A. *J. Electroanal. Chem.* **1999**, *461*, 14.
4. Varcoe, J. R.; Slade, R. C. T. *Fuel Cells* **2005**, *2*, 187.
5. Wang, J. H.; Li, S. H.; Zhang, S. B. *Macromolecules* **2010**, *43*, 3890.
6. Neburchilov, V.; Martin, J.; Wang, H. J.; Zhang, J. J. *J. Power Sources* **2007**, *169*, 221.
7. Park, J. S.; Park, S. H.; Yim, S. D.; Yoon, Y. G.; Lee, W. Y.; Kim, C. S. *J. Power Sources* **2008**, *178*, 620.
8. Wang, G. G.; Weng, Y. M.; Chu, D.; Chen, R. R.; Xie, D. *J. Membr. Sci.* **2009**, *332*, 63.
9. Fang, J.; Shen, P. K. *J. Membr. Sci.* **2006**, *285*, 317.
10. Wang, G. G.; Weng, Y. M.; Chu, D.; Xie, D.; Chen, R. R. *J. Membr. Sci.* **2009**, *326*, 4.
11. Xu, T. W.; Zha, F. F. *J. Membr. Sci.* **2002**, *199*, 203.
12. Wu, L.; Xu, T. W. *J. Membr. Sci.* **2008**, *322*, 286.
13. Xiong, Y.; Fang, J.; Zeng, Q. H.; Liu, Q. L. *J. Membr. Sci.* **2008**, *311*, 319.
14. Xiong, Y.; Liu, Q. L.; Zhang, Q. G.; Zhu, A. M. *J. Power Sources* **2008**, *183*, 447.
15. Xiong, Y.; Liu, Q. L.; Zhu, A. M.; Huang, S. M.; Zeng, Q. H. *J. Power Sources* **2009**, *186*, 328.
16. Murugesan R.; Subramanian, E. *Mater. Chem. Phys.* **2002**, *77*, 860.
17. Ramya, C. S.; Savitha, T.; Selvasekarapandian, S.; Hirankumar, G. *Ionics* **2005**, *11*, 436.
18. Fang, J.; Shen, P.K.; Liu, Q.L. *J. Membr. Sci.*, **2007**,*293*, 94.